Journal of Engineering Science and Technology
ICIST2024, Vol. 20, No. 5 (2025) 117 - 130

EFFECTS OF SWEPT BACK AND TWIST ANGLE ON THE USE OF WING AIRFOIL NACA 20612 TO AERODYNAMIC PERFORMANCE

SETYO HARIYADI SURANTO PUTRO[1,2,*], BAMBANG JUNIPITOYO[1], DANIEL D. RUMANI[2], SUTARDI[3], WAWAN ARIES WIDODO[3]

[1]Department of Aircraft Maintenance Engineering, Politeknik Penerbangan Surabaya, Jemur Andayani I/73, Wonocolo, Surabaya, Indonesia 60236
[2]Department of Aircraft Operation, Akademi Penerbang Indonesia Banyuwangi, Jalan Pantai Blimbingsari, Kelurahan Blimbingsari, Kec. Blimbingsari Kab. Banyuwangi, 68462
[3]Department of Mechanical Engineering, Faculty of Industrial Technology and Systems Engineering, Institut Teknologi Sepuluh Nopember, Jl. Arief Rahman Hakim, Surabaya, Indonesia 60111
*Corresponding Author: setyohariyadi@icpa-banyuwangi.ac.id

Abstract

The use of twist angle on the wing has been used on almost all aircraft wings. The purpose of using this configuration is to delay wingtip stall and even out the lift distribution. The effect of twist angle will be different on different airfoils and wings, especially on the aerodynamic performance of the wing. This research discusses the effect of twist angle on swept back wing compared to rectangular wing or plain wing. This research was conducted because currently the NASA 20612 used on the Embraer 145 aircraft does not use the twist angle. Numerical simulations were carried out with K-ε Realizable turbulent model at freestream velocity of 230 m/s. This study shows that the use of twist angle affects the lift to drag ratio where there is a reduction in the total drag coefficient using this design. In addition, the use of twist angle and swept angle in this study reduces the occurrence of induced drag coefficient and delays the occurrence of stall.

Keywords: Aerodynamics performance, Induced drag, NASA 20612, Swept back, Twist angle.

1. Introduction

The wing design on an airplane determines the aerodynamic performance of the entire aircraft. This is because most of the lift force is generated on the part. The amount of lift and drag greatly affects the aerodynamic performance during take-off, cruising, and landing. Each wing configuration is different on flight conditions depending in the design set by the aircraft manufacturer.

One of the other things that determine the performance of an airplane is the selection of the wing shape. Experts have introduced various wing shapes to create the best aerodynamic performance. Some common wing shapes have been introduced by several experts such as rectangular, circular, semi-circular, swept back, and others [1, 2]. These shapes are still varied with several other variables such as dihedral angle, twist angle, and others.

With these variations, the aerodynamic characteristics of the wing can of course change. With a different wing planform followed by a different wing arrangement, plus adding high lift devices, the aerodynamic performance of a wing will be quite different compared to the initial design of a wing. This leads to experts competing to modify the wing for the best aerodynamic performance.

For wing design, of course, it cannot be separated from research on wing planforms including by Khan and Al-Faruk [3], Hariyadi et al. [4], Torrigiani et al. [5], Schütte and Hummel [6], Fouda and Taha [7], Jesudasan et al. [8], Son et al. [9], (Jalil et al. [10], and others. Researchers who have explored the effect of twist angle on wings include Ismail et al. [11], Kaygan and Ulusoy [12], Hussain [13], Kale, and Pendharkar [14], Karimi Kelayeh and Djavareshkian [15], Lobo Do Vale et al. [16], and others. The twist wing design is always related to the swept-back shape and has been studied by Kaygan and Ulusoy [12], Hussain [13], Karimi Kelayeh and Djavareshkian [15].

If the angle of incidence at the wingtip is lower than the wingroot on the wing, it is referred to as negative twist, simply twist, or washout. Conversely, when the incidence angle of the wingtip is higher than that of the wingroot, it is referred to as positive twist or washin. In general, negative twist is more commonly used in aircraft, reducing the angle of attack along the span. In modern aircraft, the airfoil used at the wingroot is different from that used at the wingtip which causes a difference in the zero-lift angle of attack. This is referred to as an aerodynamic twist. This is caused when the incidence angles at the wingtip and wingroot are different, it refers to geometric twists while when the airfoils used at the wingtip and wingroot are different, it refers to aerodynamic twists.

According to Sadraey [17], the main purpose of using a twist angle in wing design is to avoid wingtip stalls before wingroot stall and modify lift distribution so that the graph is more optimally elliptical. However, there is a disadvantage of using twist angle which is the reduction of lift. The effect of this use is of course different between one type of airfoil and another airfoil, one wing shape and another wing shape.

Hussain [13] investigated the wing with NACA 2412 airfoil at twist angles of 1^{o}, 2^{o}, and 4^{o} and swept angle of 30^{o}. Computational fluid dynamic was performed on a UAV with a velocity of 0.6 Mach. The wing with a twist angle results in a

decrease in downwash velocity referring to a higher-pressure distribution. In addition, an adequate twist angle will increase lift and significantly decrease drag.

Karimi Kelayeh and Djavareshkian [15] examined the effect of twist angle variation on aerodynamic coefficient using numerical simulation. This research is based on the Reynolds-Averaged Navier-Stokes (RANS) equations using the turbulent k-ω Shear Stress Transport (SST) model for a flow speed of 30 m/s and a Reynolds number of 69000. The geometric twist was performed on a wing with NACA66009 airfoil with a swept angle of 56° at twist angles of 0°, 3°, and 6°. The effect of twist angle increases as the angle of attack increases and reaches the highest effect at the angle of attack $\alpha = 5^{o}$ which is referred to as the neutral threshold angle. With the use of a twist angle, the longitudinal stability shows satisfactory results and there is a delay in the pitch-up effect.

Kale and Pendharkar [14] conducted research on the effect of twist angles on blended wing body aircraft. The computational fluid dynamic was performed on a blended wing body model with HS-522 airfoil and velocity of 25 m/s and 30 m/s. The sweep angle used was 60° and the twist angle -3° to 3° with a step difference every 1°. The maximum lift coefficient was achieved at a twist angle of -3° and the drag coefficient was achieved at a twist angle of 1°. With an increase in twist angle, the increase in lift coefficient is higher than the increase in drag coefficient.

This study compares three configurations of NASA 20612 airfoil, namely a plain wing, a swept-back wing with twist variation, and without twist angle. NASA 20612 airfoil is used on Embraer 145 aircraft made by Embraer Brazil which is more widely used in South America and North America. This research was conducted to see the potential for improving the performance of the NACA 20612 wing used on the Embraer 145 aircraft by using a twist angle. This is very interesting because the aircraft wing currently does not use a twist angle. This study uses Computational Fluid Dynamic (CFD) numerical simulation at cruising velocity so that it can approach real conditions in flight. By demonstrating the potential for improved aerodynamic performance, there is a possibility of saving aircraft operations by modifying the wing design.

2. Methods

This research was conducted using numerical simulation, often known as Computational Fluid Dynamics. With Computational Fluid Dynamic (CFD), high Reynolds number velocities can be simulated more effectively. Conditions that cannot be achieved using laboratory experiments can be precisely implemented.

2.1. Mathematical model

According to Sadraey [17], the limitations of using the twist angle are as follows:

$$|\alpha_t| + i_w \geq |\alpha_0| \quad (1)$$

where

α_t = simply twist or twist angle

i_w = angle incidence at wing root

α_0 = zero-lift angle of attack

According to Sadraey [17], the recommended negative twist is between $\alpha_t = 1^o$ - 4^o while according to Kundu [18], the recommended negative twist is $\alpha_t = 1^o$ - 2^o and $\alpha_t = 3^o$ but should be avoided. The calculation of aerodynamic performance is based on Aselin [19] and Dole et al. [2], where the relationship between drag and lift is calculated as follows:

$$C_{Di} = KC_L^2 \quad (2)$$

$$C_D = C_{D0} + KC_L^2 \quad (3)$$

$$C_D = C_{Dmin} + K(C_L + C_{L0})^2 \quad (4)$$

$$K = \frac{1}{\pi ARe} \quad (5)$$

where:

C_{Di} = induced drag coefficient

C_L = lift coefficient

C_{D0} = pressure drag plus friction drag

AR = aspect ratio

e = Oswald efficiency factor for straight-wing aircraft

2.2. Research model

This research model uses the NASA 20612 wing airfoil used on the Embraer 145 aircraft. The simulation domain is based on the research of Mulvany et al. [20] which was continued by the research of Setyo Hariyadi et al. and Putro et al. [21, 22] by sampling the area behind the wing model five times the chordline. The application used is Ansys 19.1 with the K-ε Realizable turbulent model. The NASA 20612 airfoil can be seen in Fig. 1, and Test model specifications can be seen in Table 1.

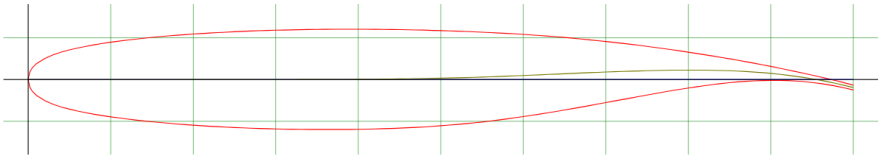

Fig. 1. Airfoil NASA 20612 (rendering result of Airfoiltools.com).

Table 1. Test model specifications.

Properties	Description
Model	3D, Unsteady Plain Wing Swept Back $\Lambda = 15^o$ Swept Back $\Lambda = 15^o$ with twist angle
Airfoil	NASA 20612
Reynolds number	$Re = 3.76 \times 10^5$
Angle of attack	0^o, 2^o, 4^o, 6^o, 8^o, 10^o,12^o,15^o, 16^o,17^o,19^o and 20^o
Twist angle	$\mu = 2^o$

3. Validation with Grid Independence

CFD requires support to ensure that the results achieved are close to the actual conditions. Grid independence is used to ensure that the mesh used has sufficient validity to show the correct values and visualization. This study used several meshes on a wing with NASA 20612 airfoil with angle of attack $\alpha = 0^o$. The validation of the study is based on Anderson [23] where the difference in C_D results from the optimal mesh is approximately 2%. In addition, the area condition used is y^+ which is less than 1 as Kontogiannis et al. [24, 25]. The details of grid independence are shown in Table 2. Considering the previous research conditions, the mesh that will be used is Mesh B.

Table 1. Three dimensional wing airfoil NASA 20612 grid independence analysis.

Number of *Mesh*	Number of Node	C_D	y^+	Skewness Average
Mesh A	862.642	0.297	0.257	0.311
Mesh B	832.000	0.216	0.176	0.314
Mesh C	706.906	0.19	0.145	0.328
Mesh D	639.000	0.15	0.11	0.343
Mesh E	504.086	0.08	0.04	0.336

4. Results

The result of this research is the aerodynamic performance in the form of drag coefficient which consists of skin friction drag, pressure drag, and induced drag. It also includes the lift coefficient so that the lift to drag ratio can be calculated. In addition, the results are also supported by visualization of the pressure coefficient on the upper surface of the wing and tip vortex in the area behind the wing.

4.1. Aerodynamic performance

The aerodynamic performance intended here is based on the understanding conveyed by Dole et al. [2] and [18, 26] where the total drag consists of skin friction drag, pressure drag, and induced drag. Meanwhile, the lift to drag ratio is the ratio between the lift coefficient and the total drag coefficient.

4.1.1. Friction drag coefficient

Figure 2 shows the friction drag coefficient of the research results. From these results, it is found that the swept-back wing configuration produces a higher skin friction coefficient than other configurations. This is influenced by the surface area of each configuration although the value of the skin friction coefficient is relatively smaller than other types of drag [22, 27, 28].

4.1.2. Pressure drag coefficient

Figure 3 shows the pressure drag coefficient of the research results. In this figure, it is found that there is no significant difference in the pressure drag coefficient results at all angles of attack except at $\alpha = 17^o$ where there is a slight decrease in the swept back wing configuration.

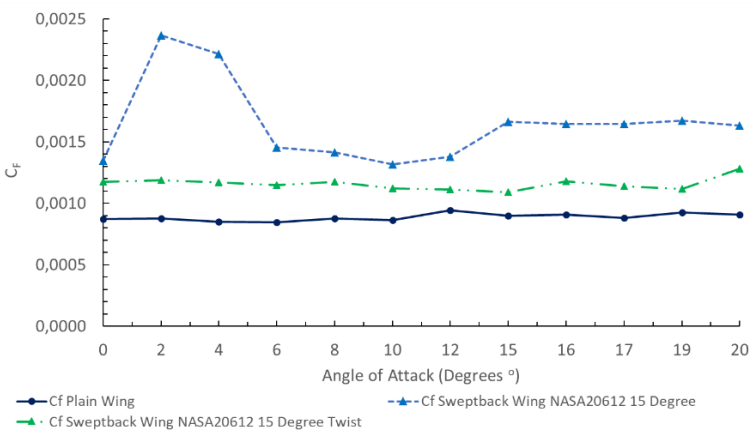

Fig. 2. Friction drag coefficient.

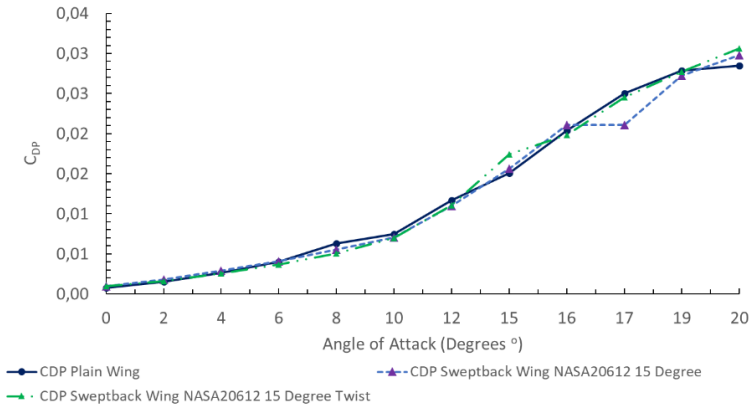

Fig. 3. Pressure drag coefficient.

4.1.3. Induced drag coefficient

Figure 4 shows the induced drag coefficient results of the research. From the Fig. 4, it is found that each configuration shows results that are different from the previous two types of drag. The swept-back wing configuration shows a continuous increase in induced drag as the angle of attack increases while the swept-back wing configuration with a twist angle shows the lowest results compared to the other configurations.

4.1.4. Total drag coefficient

Figure 5 shows the results of the total drag coefficient from the research results. Figure 5 shows that the swept-back wing configuration produces the highest value compared to other configurations while the swept-back wing configuration with twist angle produces the lowest total drag coefficient value. In addition, from the total drag coefficient value, it is found that the pattern of the value obtained is not much different from the induced drag coefficient value because this type of drag is the largest contributor to the total drag coefficient value as stated by Hariyadi et al. and SP et al. [29-31].

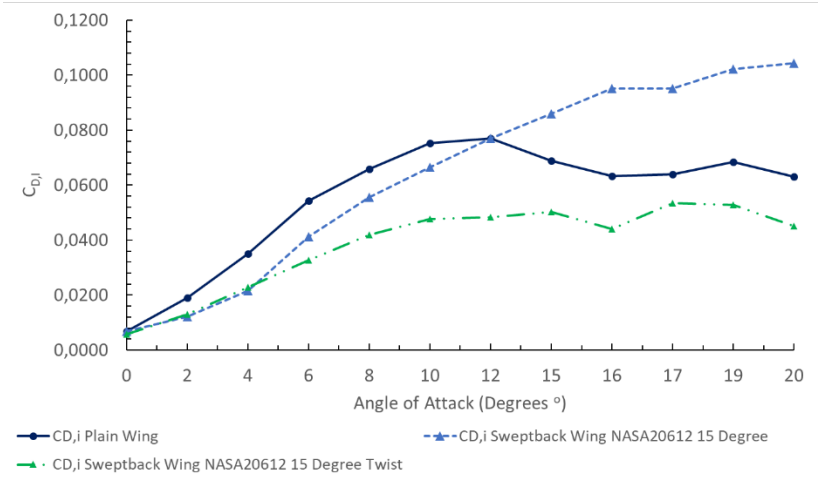

Fig. 4. Induced drag coefficient.

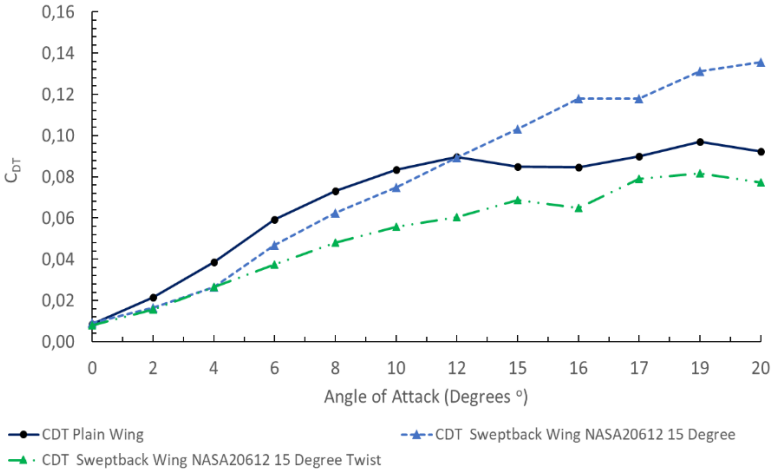

Fig. 5. Total drag coefficient.

4.1.5. Lift coefficient

Figure 6 shows the lift coefficient of the results of the study. Figure 6 shows the plain wing configuration experiences a stall at $\alpha = 12^{o}$ while the swept-back wing configuration experiences a stall at $\alpha = 16^{o}$ and the swept-back wing configuration with a twist angle experiences a stall at $\alpha = 15^{o}$. Figure 6 also shows that the swept-back wing configuration has the highest lift coefficient value compared to other configurations while the plain wing configuration produces the lowest lift coefficient value.

4.1.6. Lift to drag ratio

Figure 7 shows the results of the lift to drag ratio from the research results. Figure 7 shows that the swept-back wing configuration with a twist angle has the highest value compared to other configurations while the plain wing configuration

produces the lowest value. Figure 7 shows that the swept-back shape with a twist shape can provide the best aerodynamic performance so that it can save fuel by modifying the wing shape [32].

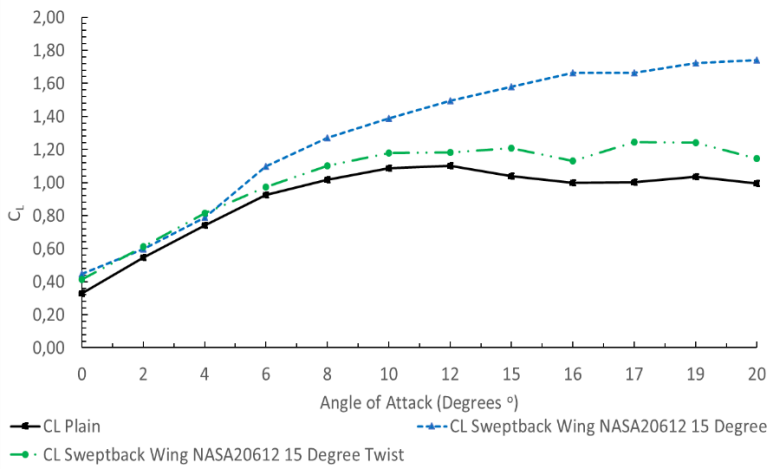

Fig. 6. Lift coefficient.

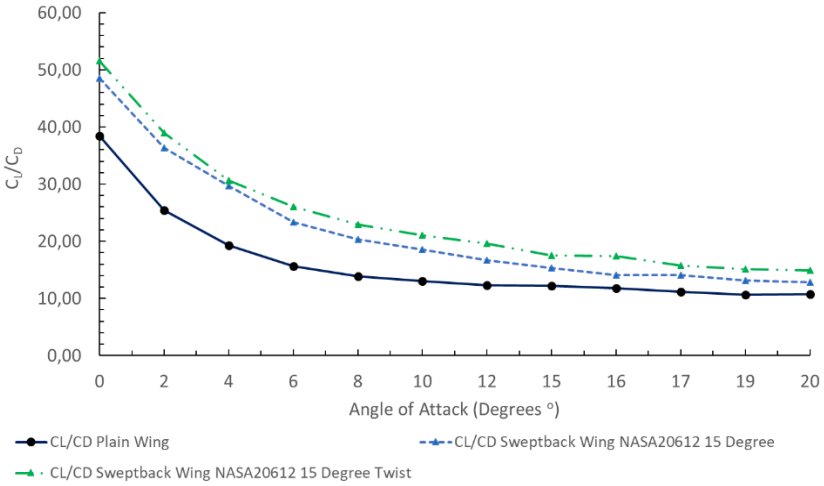

Fig. 7. Lift to drag coefficient.

4.2. Pressure Contour Visualization

Figure 8 shows the visualization of the pressure contours on the upper surface of all study configurations. Figures 8(a), (b), and (c) show the evolution of separation on the upper surface of the plain wing configuration at $\alpha = 4^o$, 10^o, and 15^o. At $\alpha = 4^o$ and 10^o, the pressure coefficient values are different at the leading edge, shoulder of wing, and trailing edge. At $\alpha = 10^o$ the pressure coefficient value appears to vary more so that at $\alpha = 15^o$ the value appears to be dominated by one value at the trailing edge to the area behind the leading edge. In conditions where a large area already has the same pressure coefficient value, it indicates that a stall has occurred in the configuration.

Figures 8(d), (e), and (f) show the evolution of separation on the upper surface of the swept-back wing configuration at $\alpha = 4^o$, 10^o, and 15^o. In the three attacks, it can be seen that the pressure coefficient values vary in all areas from wingroot to wingtip and from leading edge to trailing edge. From this display, it is found that in the area from the leading edge to the trailing edge, a stall has not occurred even though the separation gradually moves from the trailing edge to the leading edge.

Figures 8(g), (h), and (i) show the evolution of separation on the upper surface of the swept back wing configuration with a twist angle at $\alpha = 4^o$, 10^o, and 15^o. The condition on the upper surface of the swept-back wing configuration with twist angle is similar to the condition of the swept-back wing configuration where there is a variation in the contour value of the pressure coefficient from the leading edge to the trailing edge. This indicates that a stall has not occurred in this configuration.

In the wingtip region of all configurations, it can be seen that the traces of downwash occur more clearly in the plain wing configuration at all angles of attack. In the swept-back wing configuration both without and with twist angle, it can be seen that the traces of downwash only occur at $\alpha = 4^o$ and 10^o. From Fig. 8, it can be shown that the separation process is not uniform in all configurations. In the plain wing, flow separation tends to start from the wingtip area while in the swept-back wing it starts from the wingroot area.

4.3. Tip vortex visualization

Figure 9 shows the visualization of vorticity magnitude indicating the presence of tip vortex at the trailing edge of NASA 20612 $\alpha = 15^o$ in all study configurations. In the plain wing configuration (a), it can be seen that behind the wingtip has a higher value than other areas behind the trailing edge. It is known that behind the trailing edge of the plain wing configuration, there are also trailing edge vortices that stretch from the area behind the wingroot to the wingtip. This shows that in the area behind the wingtip, there is a tip vortex whose value is higher than in other areas. The tip vortex value decreases as the observation area gets further away from the wing.

In the swept-back wing configuration with and without twists angle ((c) and ((b)), it can be seen that the tip vortex value tends to be lower than that in the plain wing configuration even though the area is larger. The tip vortex value also decreases as the observation area gets further away from the wing. In the area behind the trailing edge, there are also no trailing edge vortices as occurs in the plain wing configuration.

The value of the induced drag coefficient is highly dependent on the value of the lift coefficient because the magnitude of the induced drag coefficient is proportional to the lift coefficient [1]. This phenomenon is supported by the visualization of traces of downwash in the wingtip area which shows that the induced drag coefficient that occurs on the plain wing is greater than the other configurations. In addition, the traces of downwash are greatly reduced in the swept-back configuration as stated by Raymer [33] where this shape will reduce the occurrence of tip vortex which will ultimately reduce induced drag [34]. This is supported by the reduced value of vorticity magnitude which is getting smaller in the wingtip area which indicates that the tip vortex generated is getting smaller.

The use of a twist angle has less effect on reducing the total drag coefficient and increasing the lift coefficient but has a clear impact on the lift to drag ratio. In this

study, it is shown that the use of a twist angle produces the best lift to drag ratio compared to other configurations. This shows that using the right twist angle will improve efficiency at constant speed or usually occurs in cruising conditions.

The configuration without twist angle does not mean that it has less effect on wing performance but can be used in more appropriate conditions. This can be seen in the highest lift coefficient value compared to other configurations. The most appropriate conditions are used during take-off which requires the requirement to reach the altitude value as quickly as possible compared to other configurations. This of course will have an impact on the economic aspects of the aircraft where most of the lift occurs on the wing.

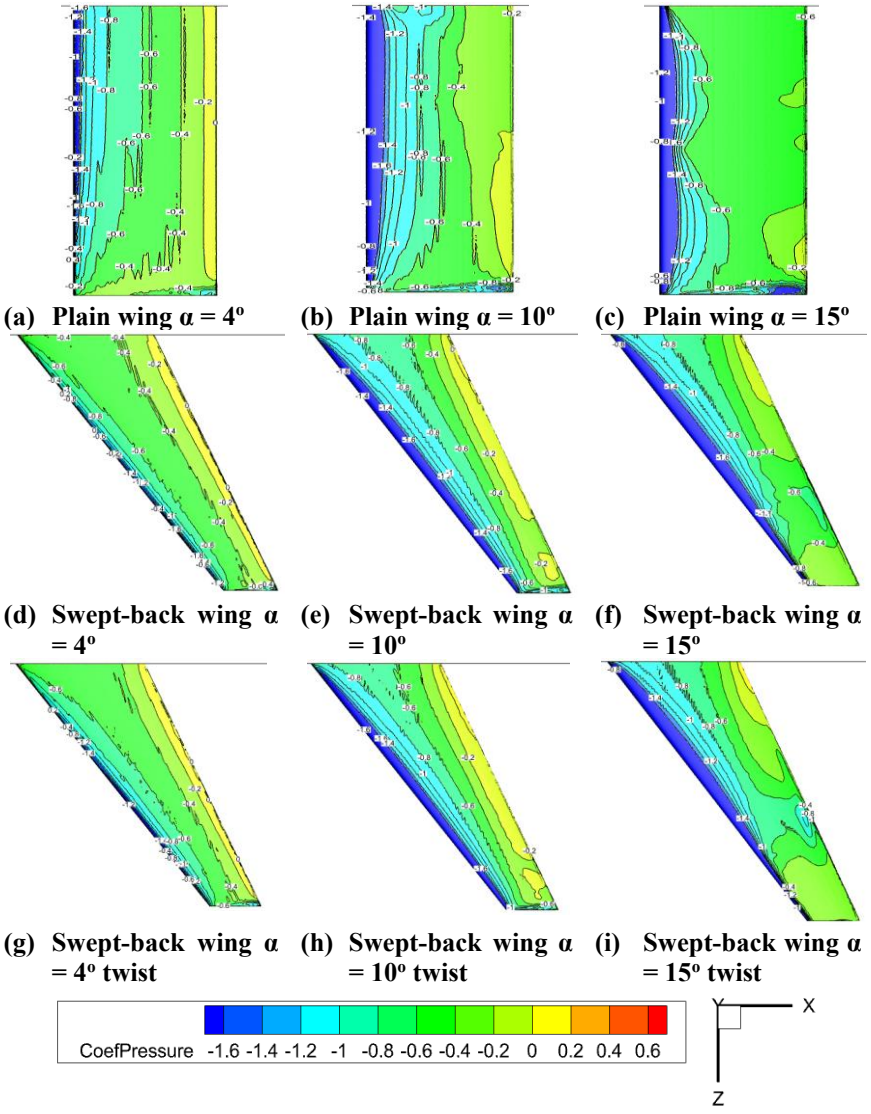

Fig. 8. Pressure coefficient visualization NASA 20612.

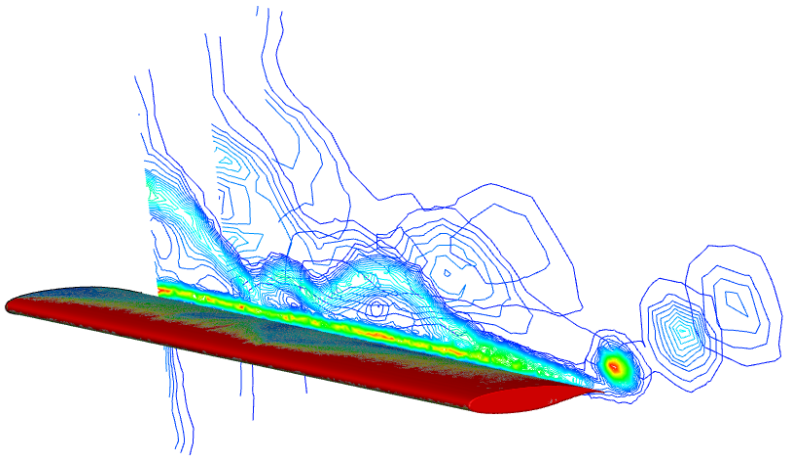

(a) Plain wing

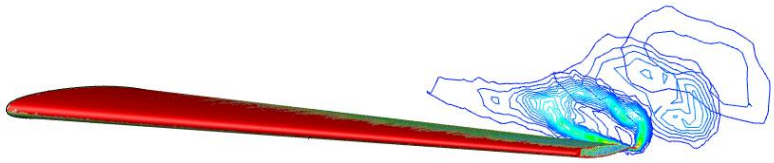

(b) Swept-back wing

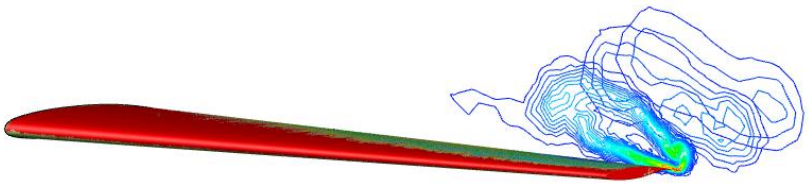

(c) Swept-back wing twist

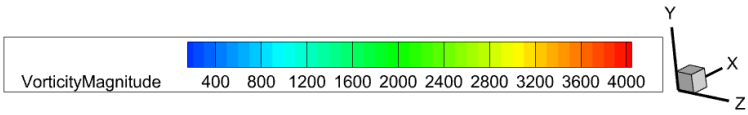

Fig. 9. Vorticity magnitude visualization NASA 20612 α = 15°.

5. Conclusions

A numerical simulation investigation on the use of twist angle has been conducted in this study. The use of a twist angle affects the lift to drag ratio although the results shown in the total drag coefficient and lift coefficient are not very significant. Twist angle in the wing airfoil NASA 20612 produces the lowest total drag coefficient

value compared to other configurations. Visualization of tip vortex supports the induced drag reduction that occurs in the swept-back wing configuration where the resulting value is lower than the plain wing configuration even though the area generated in the area behind the wingtip is wider.

The trace of down wash is clearly visible in the plain wing configuration at all angles of attack but in the swept-back wing configuration, it only occurs at low angles of attack. At high angles of attack, the downwash phenomenon is no longer visible on the wingtip. This shows that with a swept-back configuration either with a twist design or not can reduce the occurrence of induced drag which is characterized by a reduction in tip vortex. The use of the swept-back wing configuration has also effectively delayed the occurrence of stall where the plain wing configuration occurs at $\alpha = 12^{o}$ while the swept-back wing configuration occurs at $\alpha = 16^{o}$ and the swept-back wing configuration with twist angle occurs at $\alpha = 15^{o}$.

This research could be further developed by adding some basic geometric variations such as dihedral angles or changing the swept angle either swept-back or swept-forward. In addition, some high lift devices can be added to the upper surface, for example vortex generators, winglets, slats, and flaps. In addition, the phase of flight can also be a differentiator for future research, for example observations on take-off and landing conditions compared to cruising conditions.

References

1. Gudmundsson, S. (2013). *General aviation aircraft design* : *Applied methods and procedures*. Butterworth-Heinemann, Elsevier.
2. Dole, C.E.; Lewis, J.E.; Badick, J.R.; and Johnson, B.A. (2017). *Flight theory and aerodynamics*: *A practical guidefor operational safety*. John Wiley &Sons, Inc.
3. Khan, M.M.I.; and Al-Faruk, A. (2018). Comparative analysis of aerodynamic characteristics of rectangular and curved leading edge wing planforms. *American Journal of Engineering Research*, 7(5), 281-291.
4. Hariyadi, S.P.S.; Junipitoyo, B.; Sutardi; and Widodo, W.A. (2022). Stall behavior curved planform wing analysis with low Reynolds number on aerodynamic performances of wing airfoil Eppler 562. *Journal of Mechanical Engineering*, 19(1), 201-220.
5. Torrigiani, F.; Nagel, B.; and Cavallaro, R. (2022). Development of an aeroelastic stability module for wing planform optimization. *Proceedings of the* 19th *International Forum on Aeroelasticity and Structural Dynamics, IFASD* 2022, Madrid, Spain.
6. Schütte, A.; and Hummel, D. (2022). Impact of planform and control surfaces on the vortical flow topology and roll stability of a multi delta wing configuration. *Proceedings of the AIAA AVIATION* 2022 *Forum*, Chicago, IL & Virtual.
7. Fouda, M.; and Taha, H.E. (2022). Effect of wing planform on airplane stability and controauthority in stall. *Proceedings of the AIAA SCITECH* 2022 *Forum*, San Diego, CA & Virtual.
8. Jesudasan, R.; Hanifi, A.; and Mariani, R. (2023). Investigating planar and nonplanar wing planform optimisation for ground effect aircraft. *Aerospace*, 10(11), 969.

9. Son, O.; Wang, Z.; and Gursul, I. (2023). Effect of wing planform on plunging wing aerodynamics. *Journal of Fluids and Structures*, 121, 103953.
10. Jalil, M.Q.; Hashim, H.S.; and Oglah, M.K. (2024). The effects of lift curve slope and lift coefficient on the wing Cessna 172S. *Proceedings of the Transport, Ecology*, *Sustainable Development*: *Eko varna* 2023, Varna, Bulgaria.
11. Ismail, N.I.; Zulkifli, A.H.; Abdullah, M.Z.; Basri, M.H.; and Abdullah, N.S. (2014). Optimization of aerodynamic efficiency for twist morphing MAV wing. *Chinese Journal of Aeronautics*, 27(3), 475-487.
12. Kaygan, E.; and Ulusoy, C. (2018). Effectiveness of twist morphing wing on aerodynamic performance and control of an aircraft. *Journal of Aviation*, 2(2), 77-86.
13. Hussain, M. (2020). Comparative Investigation of Aerodynamic Effects on Geometrically Twisted Wing using CFD. *International Journal of Scientific Research & Engineering Trends*, 6(1), 1-5.
14. Kale, S.; and Pendharkar, E. (2021). Effects of wing twist on lift and drag characteristics of blended wing body aircraft. *Journal of Physics*: *Conference Series*, 2089(1), 012024.
15. Karimi Kelayeh, R.; and Djavareshkian, M.H. (2021). Aerodynamic investigation of twist angle variation based on wing smarting for a flying wing. *Chinese Journal of Aeronautics*, 34(2), 201-216.
16. Lobo do Vale, J.; Raffaelli, J.; and Suleman, A. (2021). Experimental validation and evaluation of a coupled twist-camber morphing wing concept. *Applied Sciences*, 11(22), 10631.
17. Sadraey, M.H. (2013). *Aircraft design: A systems engineering approach*. John Wiley & Sons, Ltd.
18. Kundu, A.K.; Price, M.A.; and Riordan, D. (2019). *Conceptual Aircraft Design: An Industrial Approach*. John Wiley & Sons Ltd.
19. Asselin, M. (1997). *An Introduction to Aircraft Performance*. American Institute of Aeronautics and Astronuatics, Inc., Reston, USA.
20. Mulvany, N.; Chen, L.; Tu, J.; and Anderson, B. (2004). Steady-state evaluation of two-equation RANS (Reynolds-averaged Navier-Stokes) turbulence models for high-Reynolds number hydrodynamic flow simulations. *Dep. Defence, Aust. Gov.*, 1-54.
21. Setyo Hariyadi, S.P.; Junipitoyo, B.; Pambudiyatno, N.; Sutardi; and Widodo, W.A. (2023). Aerodynamic characteristics of fluid flow on multiple-element wing airfoil NACA 43018 with leading-edge slat and plain flap. *Journal of Engineering Science and Technology*, 18(1), 36-50.
22. Putro, S.H.S.; Junipitoyo, B.; Suyatmo; Sutardi; and Widodo, W.A. (2024). Aerodynamic and aeroacoustic study of using multiple-element-wing leading-edge slat on plain and slotted flap wing airfoil NACA 43018. *Journal of Applied Science and Engineering*, 27(10), 3293-3304.
23. Anderson Jr, J.D. (1995). *Computational Fluid Dynamics*: *The Basics with Applications*. McGraw-Hill, Inc, New York.

24. Kontogiannis, S.G.; Mazarakos, D.E.; and Kostopoulos, V. (2016). ATLAS IV wing aerodynamic design: From conceptual approach to detailed optimization. *Aerospace Science and Technology*, 56, 135-147.
25. Kontogiannis, S.G.; and Ekaterinaris, J.A. (2013). Design, performance evaluation and optimization of a UAV. *Aerospace Science and Technology*, 29(1), 339-350.
26. Kundu, A.K. (2010). *Aircraft Design*. Cambridge University Press, New York.
27. Hariyadi Suranto Putro, S.; Junipitoyo, B.; Pambudiyatno, N.; Sutardi; and Aries Widodo, W. (2023). Aerodynamic characteristics of fluid flow on multiple-element wing airfoil NACA 43018 with leading-edge slat and plain flap. *Journal of Engineering Science and Technology*, 18(1), 36-50.
28. Suranto Putro, S.H.; Sutardi, S.; Widodo, W.A.; Pambudiyatno, N.; and Sonhaji, I. (2022). Effect of leading-edge gap size on multiple-element wing NACA 43018. *International Review of Aerospace Engineering* (*IREASE*), 15(6), 321-331.
29. Hariyadi, S.S.; Widodo, W.A.; and Mustaghfirin, M.A. (2018). Aerodynamics analysis of the wingtip fence effect on UAV wing. *International Review of Mechanical Engineering* (*IREME*), 12(10), 837-846.
30. Hariyadi, S.P.S.; Pambudiyatno, N.; Sutardi; and Fungky Dyan, P. (2023). *Aerodynamic characteristics of the wing airfoil NACA* 43018 *in take off conditions with slat clearance and flap deflection*. In Tolj, I.; Reddy, M.V.; and Syaifudin, A. (Eds.), *Recent Advances in Mechanical Engineering*. Springer Nature Singapore, 220-229.
31. SP, S.H.; Junipitoyo, B.; Ali, S.; and Widodo, W. A. (2022). Stall Behavior Curved Planform Wing Analysis with Low Reynolds Number on Aerodynamic Performances of Wing Airfoil Eppler 562. *Journal of Mechanical* Engineering, 19(1), 201-220.
32. Gavrilović, N.N.; Rašuo, B.P.; Dulikravich, G.S.; and Parezanović, V.B. (2015). Commercial aircraft performance improvement using winglets. *FME Trans.* 43, 1-8.
33. Raymer, D.P. (1992). *Aircraft design*: *A conceptual approach*. American Institute of Aeronautics and Astronautics, Inc.
34. Raymer, D. (2019) *Aircraft Design*: *A Conceptual Approach*, *Sixth Edition*. American Institute of Aeronautics and Astronautics, Inc.